Supporting Information for Tunable knot segregation in co-polyelectrolyte rings carrying a neutral segment

Andrea Tagliabue,[†] Cristian Micheletti,[*,‡] and Massimo Mella[*,†]

Dipartimento di Scienza ed Alta Tecnologia, Università degli Studi dell'Insubria, via Valleggio 11, 22100, Como, Italy, and SISSA (Scuola Internazionale Superiore di Studi Avanzati), via Bonomea 265, 34136, Trieste, Italy

E-mail: cristian.micheletti@sissa.it; massimo.mella@uninsubria.it

[*]To whom correspondence should be addressed

[†]Dipartimento di Scienza ed Alta Tecnologia, Università degli Studi dell'Insubria, via Valleggio 11, 22100, Como, Italy

[‡]SISSA (Scuola Internazionale Superiore di Studi Avanzati), via Bonomea 265, 34136, Trieste, Italy

Model and methods

The simulated system consists of a single circular co-polyelectrolyte (co-PE, or "ring") contained in a periodically repeated cubic cell of side length $L = 76.36\sigma$ ($\sigma = 3.55$ Å), the latter value chosen in order to have a molar concentration of monomers equal to $C_{\mathrm{mono}} = 10^{-2}$ M. The circular co-PE is represented via a coarse–grained "beads–springs" primitive model, and it is composed by $N = 120$ monomers, N_{neu} of which are neutral, whereas the remaining $N - N_{\mathrm{neu}}$ beads carry a quenched monovalent negative charge (*i.e.*, they act as strong electrolytes). In order to maintain the system electroneutral, in solution there are also $N_{\mathrm{CI}} = N - N_{\mathrm{neu}}$ monovalent positive counterions (CI's).

Bonds between adjacent beads are simulated via a finitely extensible non–linear elastic (FENE) potentials,[1]

$$U_{\mathrm{bond}}(r_{ij}) = -\frac{1}{2} k_{\mathrm{bond}} r_{\mathrm{max}}^2 \ln\left(1 - \left(\frac{r_{ij}}{r_{\mathrm{max}}}\right)^2\right), \tag{1}$$

where r_{ij} is the distance between two connected monomers i and j, $k_{\mathrm{bond}} = 30\epsilon/\sigma^2$ is the force constant, and $r_{\mathrm{max}} = 3\sigma$ is the maximum allowed elongation.

All particles interact via a Weeks–Chandler–Anderson (WCA) potential[2] which simulate their excluded volumes:

$$U_{\mathrm{WCA}}(r_{ij}) = \begin{cases} 4\epsilon\left[\left(\frac{\sigma}{r_{ij}}\right)^{12} - \left(\frac{\sigma}{r_{ij}}\right)^{6} + \frac{1}{4}\right] & \text{if } r_{ij} < r_{\mathrm{cut}} \\ 0 & \text{otherwise;} \end{cases} \tag{2}$$

here, r_{ij} is the distance between two interacting particle i and j, $\epsilon = k_{\mathrm{B}}T$ and σ are, respectively, the strength and the range of interaction, and $r_{\mathrm{cut}} = 2^{\frac{1}{6}}\sigma$ is the cutoff radius.

Electrostatic interactions are calculated via the P^{3}M method, with an accuracy set to 10^{-3}. The molecular structure of water is omitted, and the solvent is represented by a uniform dielectric continuum with a Bjerrum length $l_{\mathrm{B}} = 2\sigma$; setting $\sigma = 3.55$ Å thus results in the typical Bjerrum length of water at room temperature, $l_B = 7.10$ Å.

Two different knot topologies have been investigated: the "trefoil knot" (3_1, three essential crossings) and the "pentafoil knot" (5_1, five essential crossings).

Simulation protocol

Conformations at the equilibrium are sampled via Langevin dynamics according to

$$m_i \ddot{\mathbf{r}}_i = -\gamma \dot{\mathbf{r}}_i + \mathbf{F}_i + \mathbf{R}_i, \tag{3}$$

where $m_i \equiv m = 1$ (in internal units) is the mass of the i-th particle, $\dot{\mathbf{r}}$, $\ddot{\mathbf{r}}$, $\mathbf{F}_i$, and $\mathbf{R}_i$ are, respectively, its velocity, its acceleration, and the conservative and the random forces acting on it, and $\gamma = \sigma^{-1}/(m\epsilon)^{\frac{1}{2}}$ is the friction coefficient. Random forces act on each particle independently and obey the fluctuation–dissipation theorem. Equation 3 is integrated by a velocity Verlet algorithm with a time step $\delta t = 0.01\sigma(m/\epsilon)^{\frac{1}{2}}$; thus, our system time unit, $\tau_{\mathrm{MD}} = \sigma\sqrt{(m/\epsilon)}$, consists in 100 integration steps.

For each case investigated, we simulated 100 independent trajectories; hence, we present the averaged results accompanied by their standard errors. During each trajectory simulation, the system has been thermalized for a time $t_{\mathrm{therm}} = 5 \cdot 10^5 \delta t$. After the thermalization, the trajectory has been integrated for a time $t_{\mathrm{sim}} = 2 \cdot 10^6 \delta t$, during which the system properties have been collected every 10^3 time steps. All simulations have been performed with the software package ESPResSo.[3]

Knot analysis

Monomers in the ring are indexed as a function of their positional distance from the NS midpoint, δ_{NS}. Thus, $\delta_{\mathrm{NS}} = 0$ for the two (neutral) central monomer, $\delta_{\mathrm{NS}} = 1$ for their first neighbors, *etc.* Analogously, we define a similar metric, δ_{k}, in order to index the position of a bead with respect to the knot midpoint.

The knotted segments are recognized performing a bottom–up search with the software KymoKnot.[4,5] At each time $t = t_0$, we define a total ordered set $\mathbb{K}(t_0)$ containing the position index of all the monomers taking part to the chain knotted portion; from this, one can define the "knot length" ℓ_K as $\ell_\mathrm{K}(t_0) = \#\mathbb{K}(t_0)$, where "#" denotes the set cardinality. Thus, ℓ_K corresponds to the number of monomers lying in the knotted portion of the ring.

From the collected data, one can calculate the probability density $\rho(\delta_\mathrm{NS})$ for a monomer j,which lies at distance δ_NS from the NS midpoint, to be part of the knotted segment by simply dividing the number of occurrences of a given monomer j in $\mathbb{K}$ by the total number of conformations sampled. $\rho(\delta_\mathrm{NS})$ is normalized so to have $\int_0^{N/2} \rho(\delta_\mathrm{NS})\mathrm{d}\delta_\mathrm{NS} = 1$, representing *de facto* the cumulative probability for a monomer lying at a distance δ_NS to be included in the knot.

We also define as "knot midpoint" the monomer $j = j_\mathrm{mid}(t_0)$ lying in the middle of the knotted arc at $t = t_0$. If $\#\mathbb{K}(t_0)$ is odd, $j_\mathrm{mid}(t_0)$ results to be median element of $\mathbb{K}$; conversely, if $\#\mathbb{K}(t_0)$ is even we identify the "middle monomer" as the median element of the set $\#\mathbb{K}^*$, the latter a subset of $\#\mathbb{K}(t_0)$ obtained by randomly removing from the latter the first *or* the last element with an equal probability. Analogously to $\rho(\delta_\mathrm{NS})$, we define the density of probability $\rho_\mathrm{mid}(\delta_\mathrm{NS})$ for a monomer j (which lies at distance δ_NS from the NS midpoint) to be the knot midpoint. Since, also in this case, $\int_0^{N/2} \rho_\mathrm{mid}(\delta_\mathrm{NS})\mathrm{d}\delta_\mathrm{NS} = 1$, $\rho_\mathrm{mid}(\delta_\mathrm{NS})$ represents the cumulative probability to find the knot midpoint in the interval 0–NS.

Results

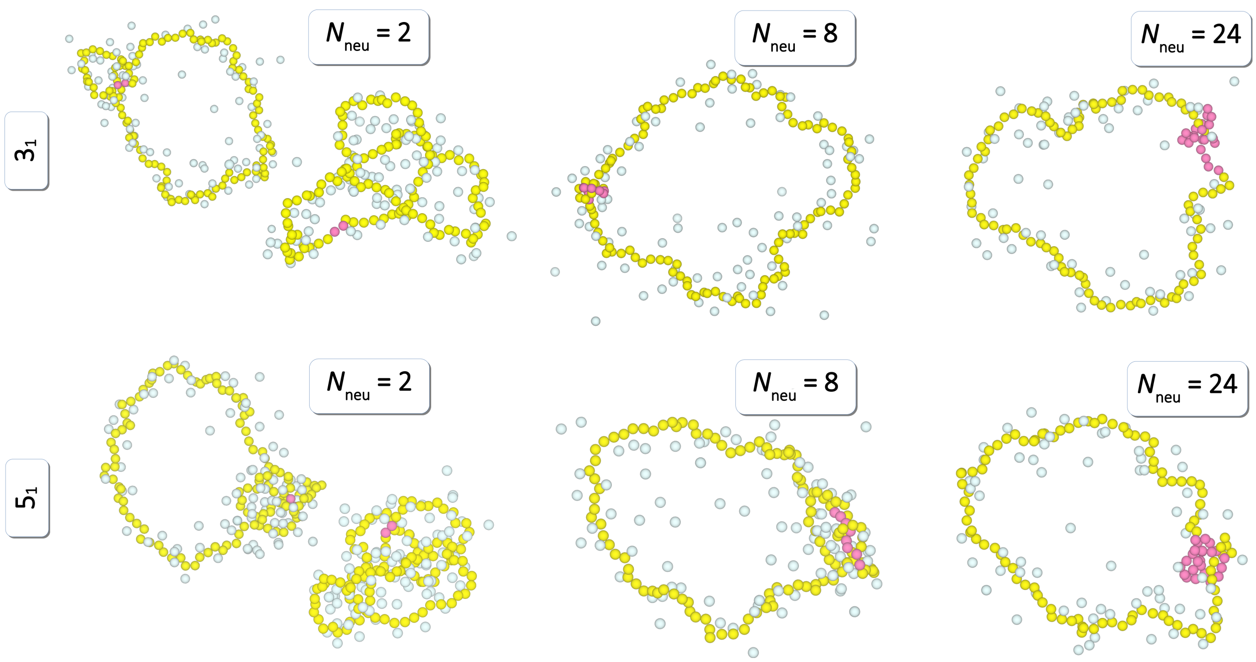

Figure S1: Selected trajectory snapshots for systems with $N_{\rm neu}$ = 2, 8, and 24. Color scheme: neutral monomers pink, charged monomers in yellow, counterions in ice blue. The color scheme is maintained through the manuscript.

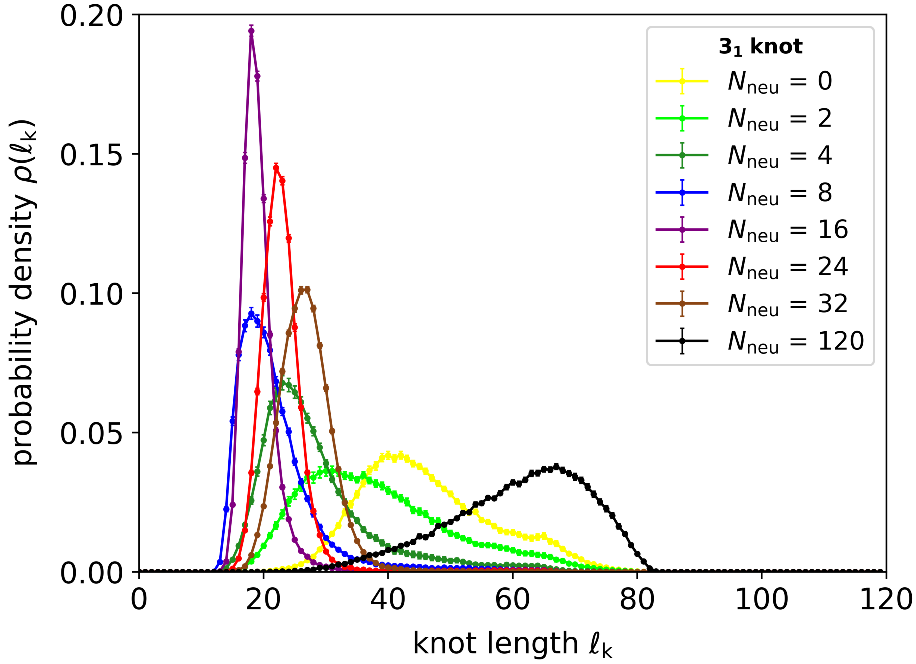

(a) 3_1 topology.

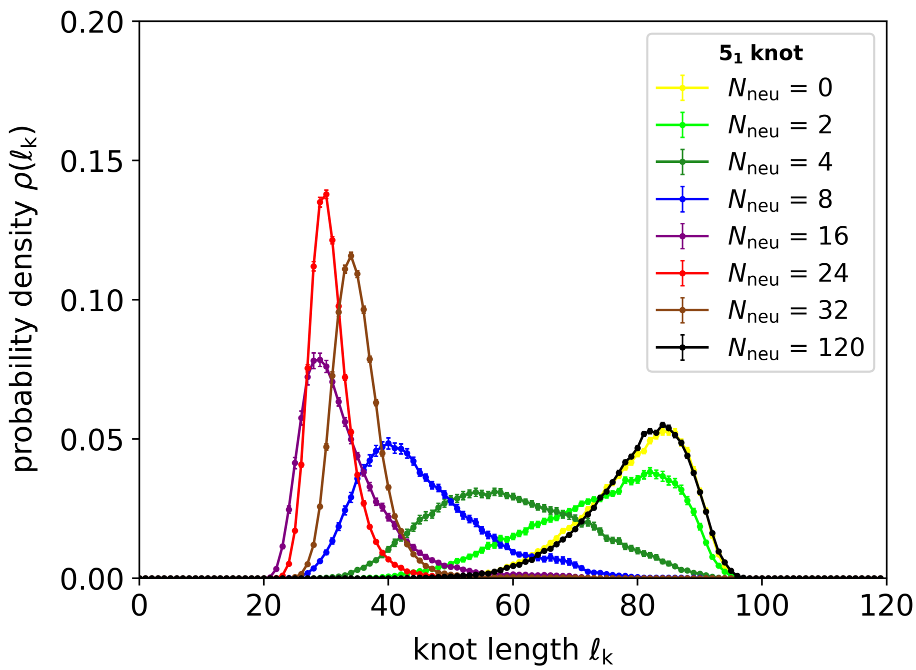

(b) 5_1 topology.

Figure S2: Probability densities to find ring conformations with a certain knot length ℓ_K.

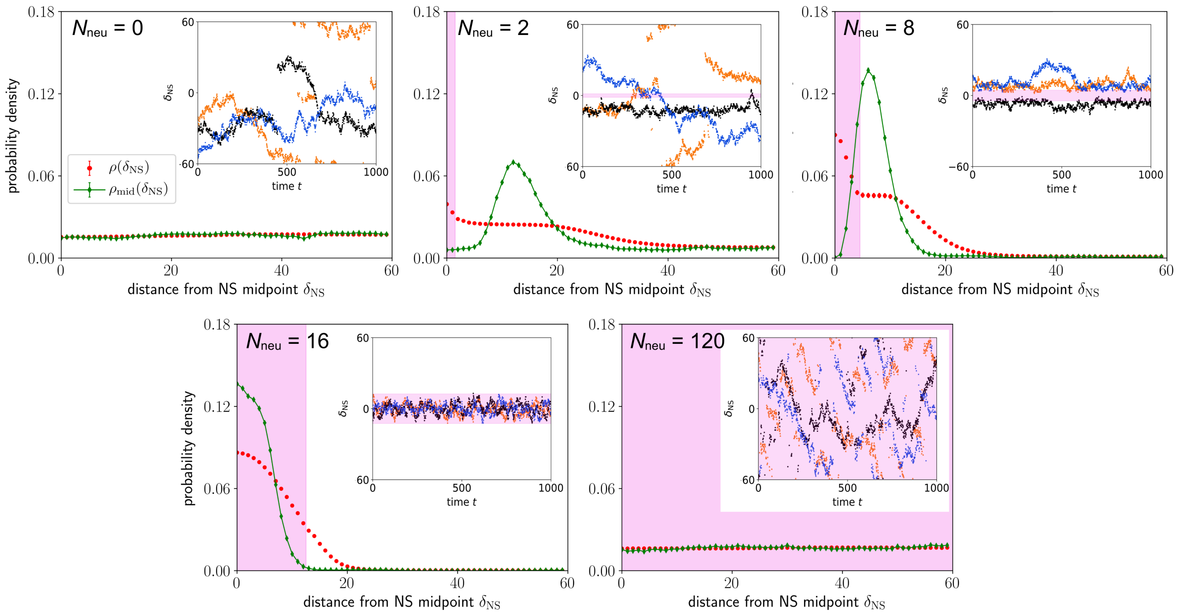

(a) 3_1 topology.

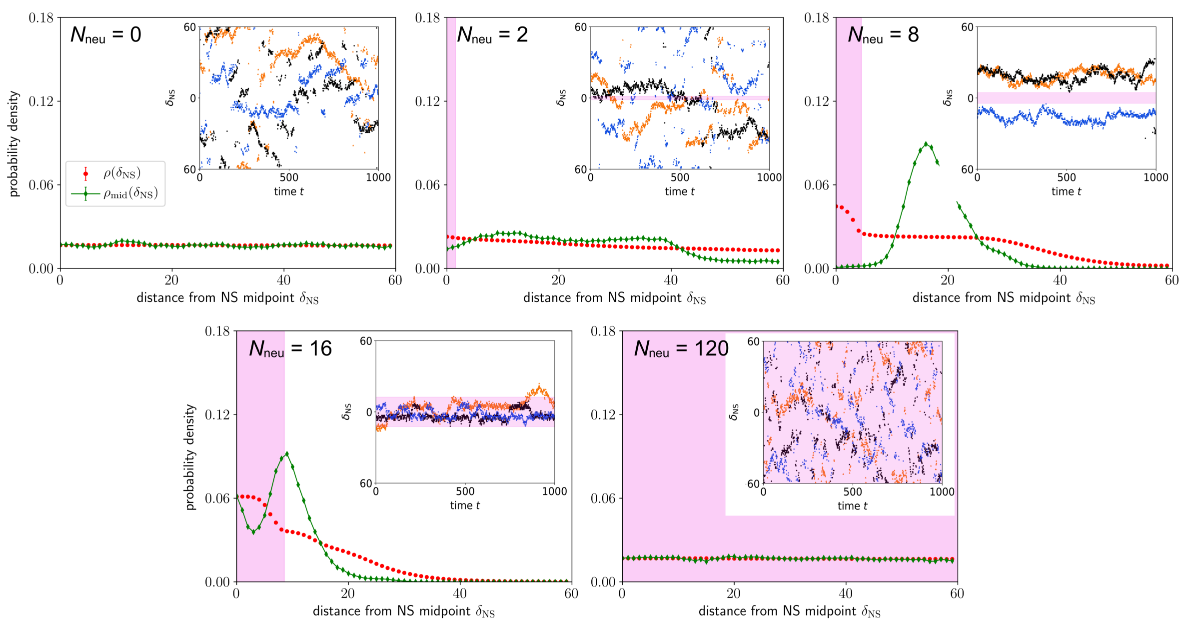

(b) 5_1 topology.

Figure S3: Probability distributions ρ and ρ_{mid} as a function the monomer distance δ_{NS} for systems with $N_{\mathrm{neu}} = 0$, 2, 8, 24, and 120. Curves have been symmetrized around the latter due to the intrinsic symmetry of the co-PE's. Each inset shows 3 independent trajectories of the contour motion of the knot midpoint. Areas highlighted in pink denotes the NS's.

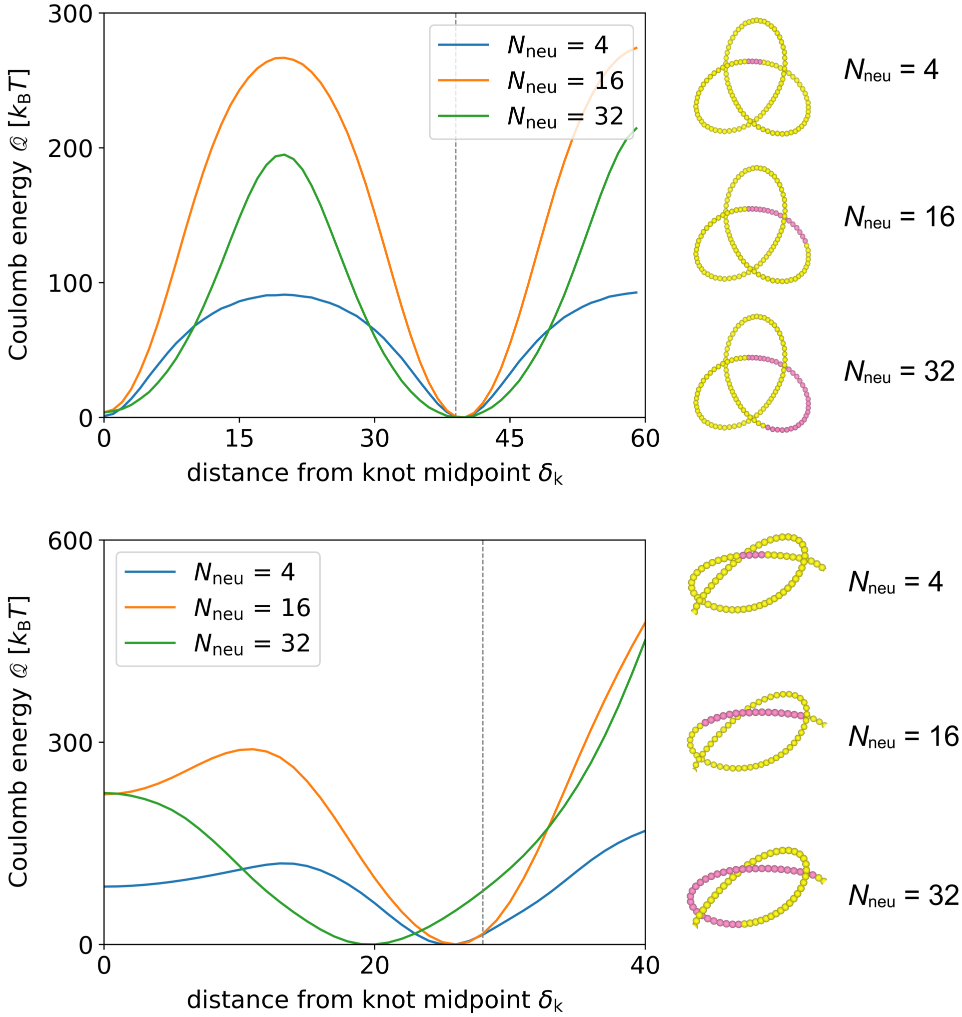

Figure S4: Coulomb energy $\mathcal{Q}$ (in $k_B T$ units) as a function of the distance δ_k between knot and NS midpoints for the 3_1 topology and N_{neu} values. Upper panel: ideal knot, $\ell_k = 78$; lower panel: $\ell_k = 75$.

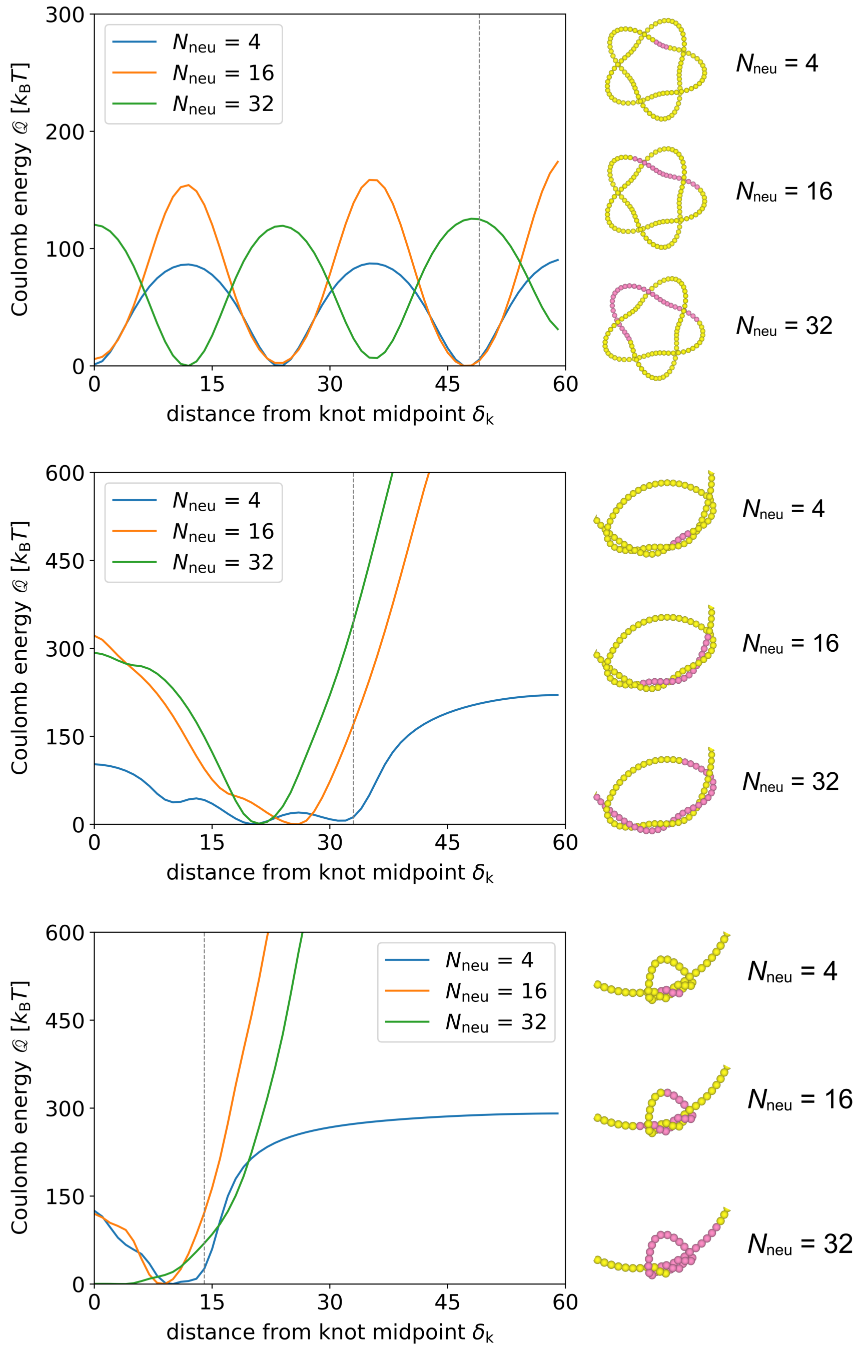

Figure S5: Coulomb energy $\mathcal{Q}$ (in k_BT units) as a function of the distance δ_k between knot and NS midpoints for the 5_1 topology and various N_{neu} values. Upper panel: ideal knot, $\ell_k = 97$; central panel: $\ell_k = 65$, lower panel: $\ell_k = 28$.

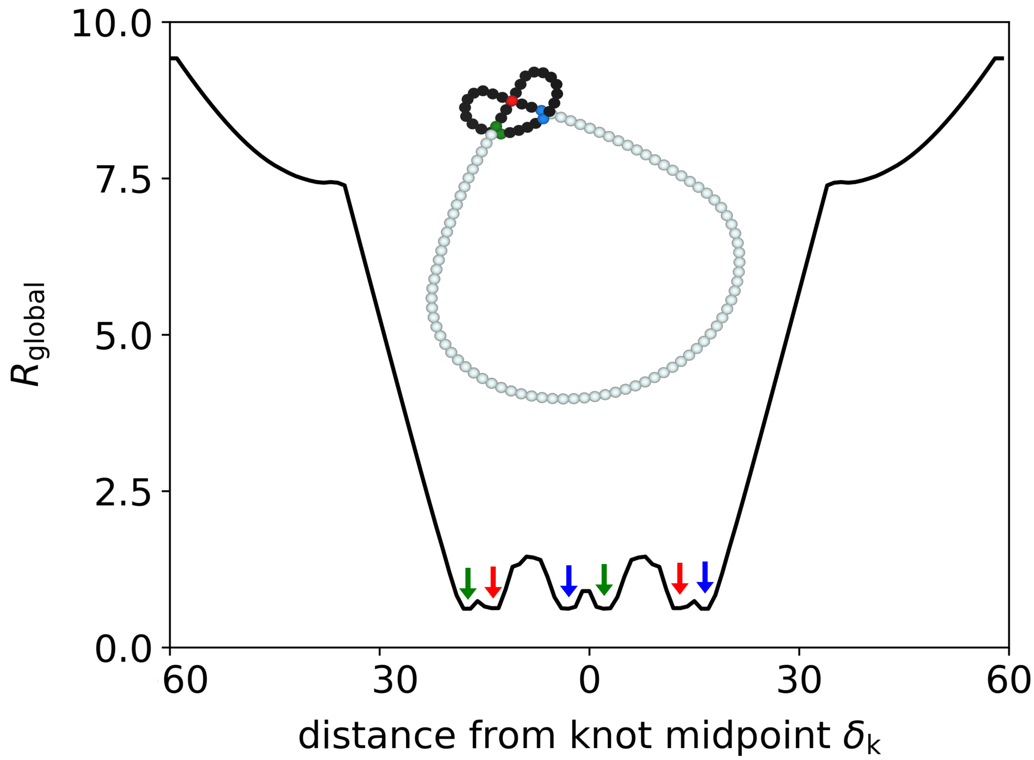

Figure S6: Global radius of curvature, $R_{\mathrm{global}} = R_c^g(i)$, as a function of the monomer index, i, of the shown trefoil-knotted ring. Following ref. 6, the global radius of curvature of monomer i is defined as $R_c^g(i) = \min j, k, j \neq k r_{ijk}$, where r_{ijk} is the radius of the circumcircle going through monomers i, j, k. The physical interpretation of $R_c^g(i)$ is that it provides the maximum thickness to which one can inflate the curve, making it into a tube of uniform cross-section before it becomes singular at i. This can occur under two circumstances, either a tight local radius of curvature at i (in which case the minimizing ijk triplet is formed by consecutive monomers) or due to the contact of the tube at i and another region away from it[6]. For rings with localized knots, the minima of the $R_c^g(i)$ profile correspond to the regions where the ring center-line is in close proximity of itself. The minima can thus be used to identify the regions defining the essential crossing, which are indicated by the colored arrows.

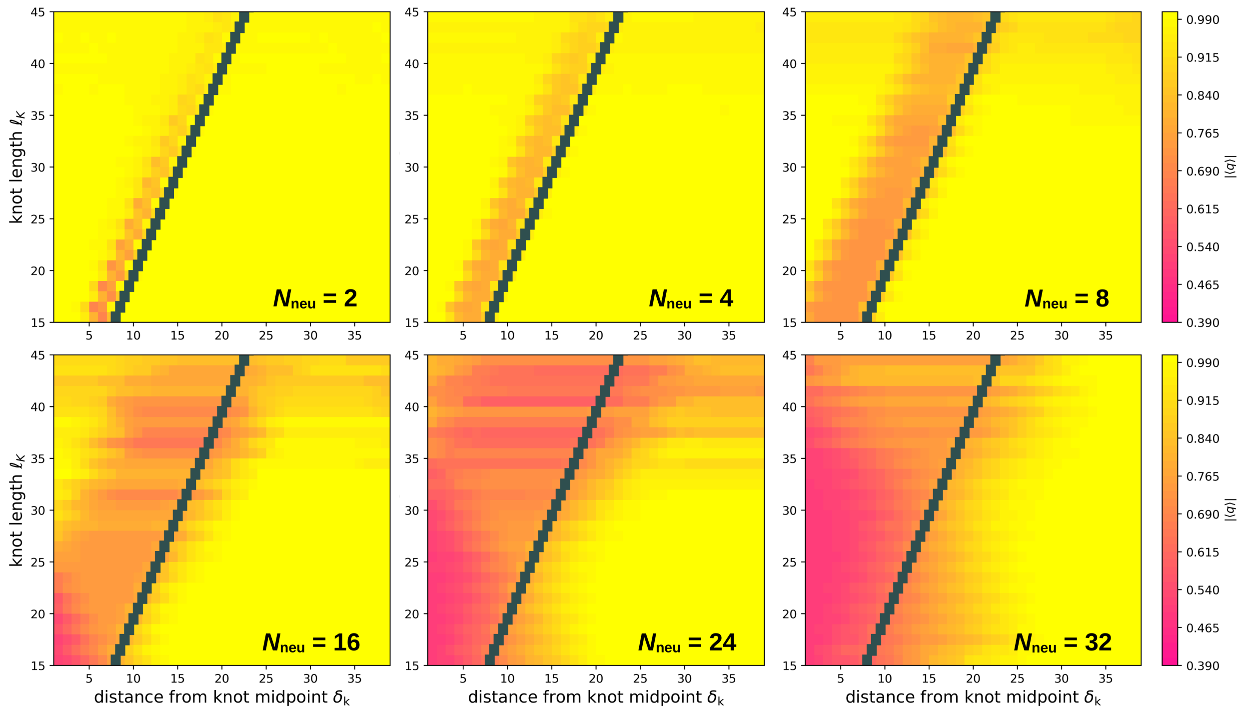

Figure S7: Unsigned average effective charge $|\langle q \rangle|$ of monomers in 3_1-knotted rings and various N_{neu}. The average is taken at various knot lengths (ℓ_{K}, y axis) and sequence distances (δ_{k}, x axis) from the knot midpoint. For reference, the $\ell_{\mathrm{K}} = 2\delta_{\mathrm{k}}$ line is superposed to the main graphs.

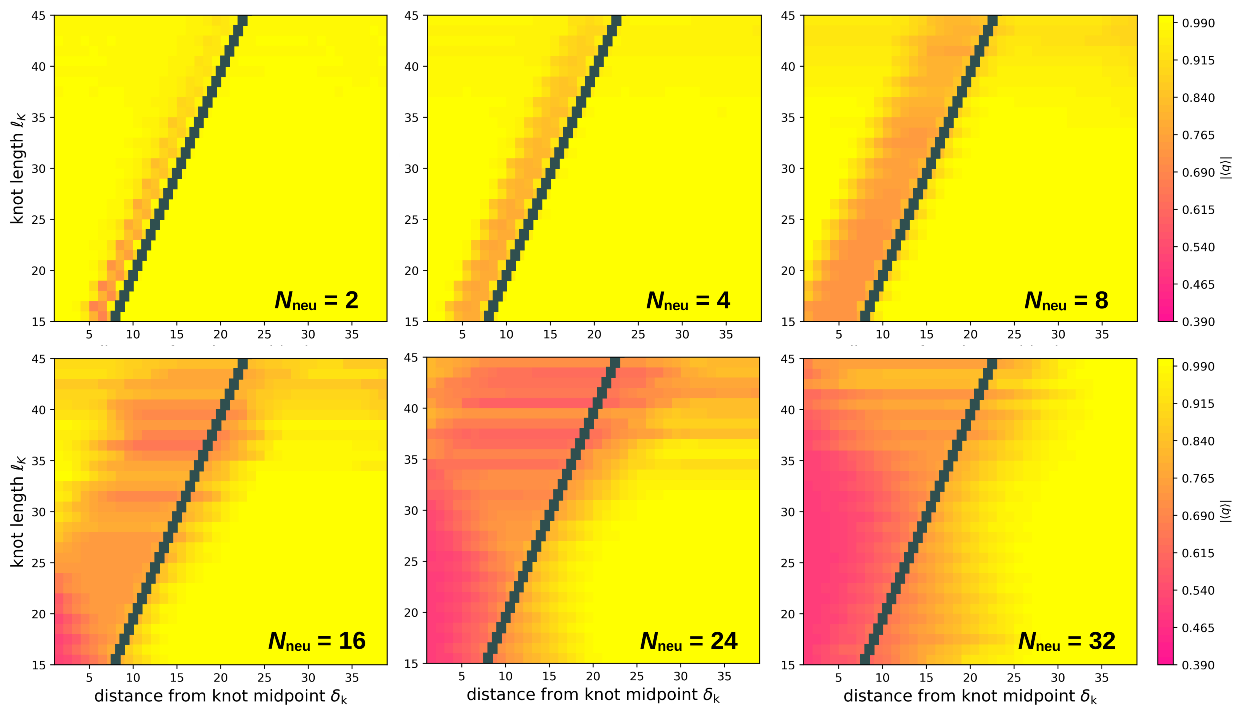

Figure S8: Unsigned average effective charge $|\langle q\rangle|$ of monomers in 5_1-knotted rings and various N_{neu}. The average is taken at various knot lengths (ℓ_{K}, y axis) and sequence distances (δ_{k}, x axis) from the knot midpoint. For reference, the $\ell_{\mathrm{K}} = 2\delta_{\mathrm{k}}$ line is superposed to the main graphs.

References

(1) Kremer, K.; Grest, G. S. Dynamics of entangled linear polymer melts: A molecular-dynamics simulation. *J. Chem. Phys.* **1990**, *92*, 5057.

(2) Weeks, J. D.; Chandler, D.; Andersen, H. C. Role of Repulsive Forces in Determining the Equilibrium Structure of Simple Liquids. *The Journal of Chemical Physics* **1971**, *54*, 5237–5247.

(3) Weik, F.; Weeber, R.; Szuttor, K.; Breitsprecher, K.; de Graaf, J.; Kuron, M.; Landsgesell, J.; Menke, H.; Sean, D.; Holm, C. ESPResSo 4.0 – An Extensible Software Package for Simulating Soft Matter Systems. *Eur. Phys. J-Spec. Top.* **2019**, *227*, 1789–1816.

(4) Tubiana, L.; Polles, G.; Orlandini, E.; Micheletti, C. KymoKnot: A web server and software package to identify and locate knots in trajectories of linear or circular polymers. *European Physical Journal E* **2018**, *41*.

(5) Tubiana, L.; Orlandini, E.; Micheletti, C. Probing the Entanglement and Locating Knots in Ring Polymers: A Comparative Study of Different Arc Closure Schemes. *Prog. Theor. Phys. Suppl.* **2011**, *191*, 192–204.

(6) Gonzalez, O.; Maddocks, J. H. Global curvature, thickness, and the ideal shapes of knots. *Proceedings of the National Academy of Sciences* **1999**, *96*, 4769–4773.